

# Artificial Intelligence-Steered Multi-Objective Design Augmentation for Yaw Bearing of Wind Turbine Electricity Generation Mechanism

Prasun Bhattacharjee<sup>1\*</sup>, Rabin K. Jana<sup>2</sup> and Somenath Bhattacharya<sup>3</sup>

<sup>1</sup>Department of Mechanical Engineering  
Ramakrishna Mission Shilpapitha  
Kolkata, West Bengal 700056 India  
<sup>\*</sup>prasunbhatta@gmail.com

<sup>2</sup>Operations & Quantitative Methods Area  
Indian Institute of Management Raipur  
Chhattisgarh 493661, India

<sup>3</sup>Department of Mechanical Engineering  
Jadavpur University  
Kolkata 700032, India

Date received: December 31, 2023

Revision accepted: November 26, 2024

---

## Abstract

*Unchecked rise in greenhouse gas emissions exacerbates global climate instability, leading to severe ecological disruptions, economic losses, and threats to human health and biodiversity. The sector of electricity is a prominent source of greenhouse gases. Power-generating companies may drastically lessen their fossil fuel consumption by exploring the use of renewable energy sources like wind power. Each year, a noteworthy amount of the functioning time of wind turbines remains unused because of mechanical breakdowns in various of its components. A crucial part of the wind turbine, the yaw bearing enables the wind turbine blades to remain in the correct alignment needed for efficient power generation. In this research, artificial intelligence methods such as the Genetic Algorithm and JAYA Algorithm have been exercised to augment the yaw bearing design. While the Bearing Frictional Torque has been taken into consideration for reduction, Basic Dynamic Axial Load Rating and Static Load Factor have been taken into account for expansion. The Multi-Objective Genetic Algorithm proves to be more advantageous than the Multi-Objective JAYA Algorithm in enhancing the wind turbine yaw bearing's operational dependability.*

**Keywords:** genetic algorithm, JAYA algorithm, multi-objective optimization  
wind turbine, yaw bearing

---

## **1. Introduction**

The continuous release of greenhouse gases into the atmosphere, resulting from various social commotions, such as unsustainable consumption of non-renewable fuels, largely contributes to unusual increase in global warming and hastening of its process (Bhattacharjee *et al.*, 2022; Obama, 2017). To prevent the climate change's disastrous effects, a record number of UN allies voted in favor of authorizing an international agreement in Paris in 2015. This agreement aims to considerably lower greenhouse gas generation by directing the responsible management of renewable energy sources, such as wind power (United Nations, 2015). A pragmatic gauge of the universal tendency toward low-carbon energy alternatives is the progressively mounting stake of renewable resources like wind power in aggregate power generation over the last three decades (International Energy Agency, 2021). Annual worldwide wind power generation swelled from 4.73 TWh in 1992 to 2098.46 TWh in 2022 (Energy Institute, 2023). Because of its outstanding dependability and inexpensive cost, renewable power sources like wind power are required to continue being sustainable in conjunction with the smallest emanation lead. As a result, appropriate attention needs to be maintained during the wind turbine design phase to reduce the chance of disruption during the operational cycle. It is clear from several earlier studies that mechanical failures cause wind turbines to lose a sizeable amount of functioning time each year all across the world (Babu and Jithesh, 2008).

Each onshore Wind Turbine (WT) has a 0.23 failure rate per year due to the yaw mechanism of the wind power-yielding system (Van Bussel and Zaaier, 2001). Researchers used the Windstats reliability records and power law technique to evaluate the failure rates of German and Danish WTs. Additionally, they noted that after seven years, the failure rates of Danish turbines will converge to those of German WTs, which had a little higher failure rate (Tavner *et al.*, 2005). Researchers used the 250 MW WT test database to analyze wind turbine breakdown. They observed that as time went on, the malfunction rates decreased (Echavarria *et al.*, 2008). Numerous characteristics of recurring flaws discovered in different WT sub-assemblies have also been examined (Yang *et al.*, 2012). It is also advised to use Permanent Magnetic Bearings (PMB) in small WT vertical axis applications. Researchers used mathematical model simulation using COMSOL Multiphysics software and finite element analysis with ANSYS. The experiment demonstrated that the vertical axis small wind turbine with PMB performed better in terms of increased turbine speed and rotation time than the

same configuration without PMB (Micha *et al.*, 2017). To estimate the WT's lifespan, a load-centered maintenance approach was put out. The impact of several factors such as blade cone angle, yaw misalignment, and gust turbulence were assessed (Rommel *et al.*, 2020).

In a WT, the yaw mechanism is operated to align the rotor with the direction of the wind flow. The WT rotor has to be kept in the airflow direction for optimal energy extraction (Wu and Wang, 2012). WT yaw bearings experience twisting moments, axial loads, and radial loads all at once. The exterior and internal raceways of the yaw bearings are shaped by two ring-rolled forged components. To transmit load and moments, the cross-roller bearing's rollers rotate in opposite directions, spaced apart by saddle-shaped spacers in WT yaw bearings (Harris *et al.*, 2009). Although various studies have explored wind turbine reliability and component performance, there remains a dearth of research on leveraging Artificial Intelligence (AI) for multi-objective optimization specifically aimed at augmenting yaw bearing design by maximizing the Basic Dynamic Axial Load Rating ( $C_a$ ), minimizing Bearing Friction Torque ( $T$ ), and maximizing Static Load Factor ( $SF$ ) using meta-heuristic techniques like the Genetic Algorithm and JAYA algorithm. This gap limits advancements in improving the durability and efficiency of wind turbine electricity generation mechanisms under complex load conditions. This research aims to optimize yaw bearing design by employing Genetic Algorithm and JAYA Algorithm, to minimize Bearing Frictional Torque while maximizing the Basic Dynamic Axial Load Rating and Static Load Factor, with a comparative analysis of the most efficient designs generated.

## **2. Methodology**

### *2.1 Basic Dynamic Axial Load Rating ( $C_a$ )*

Yaw bearings are subjected to an eccentric thrust-type force as their principal load, which results in an axial load and moment. The stable centric thrust force that a rolling element bearing may theoretically experience over a rated operating lifespan ( $L_{10}$ ) of one million revolutions is known as the basic dynamic axial load rating ( $C_a$ ). The applied radial force and its load rating are used to calculate the bearing fatigue life (Gupta *et al.*, 2007).  $C_a$  is computed as per Equation 1 (Harris *et al.*, 2009).

$$C_a = f_{cm} (l_e \cos \alpha)^{\frac{7}{9}} z^{\frac{3}{4}} D_b^{\frac{29}{27}} \tan \alpha \tag{1}$$

The geometric parameter  $f_{cm}$  can be computed as per Equation 2.

$$f_{cm} = 37.91 \left[ 1 + \left\{ 1.04 \left( \frac{1-\gamma}{1+\gamma} \right)^{1.72} \left( \frac{f_i(2f_o-1)}{f_o(2f_i-1)} \right)^{0.41} \right\}^{10/3} \right]^{0.3} \left[ \frac{\gamma^{0.3} (1-\gamma)^{1.39}}{(1+\gamma)^3} \right] \left[ \frac{2f_i}{2f_i-1} \right]^{0.41} \tag{2}$$

Another geometric factor  $\gamma$  has been calculated as per Equation 3.

$$\gamma = \frac{D_b \cos \alpha}{D_m} \tag{3}$$

Where,  $l_e$  represents the roller's effective length,  $\alpha$  signifies the contact angle,  $z$  stands for the number of rolling elements per row,  $D_b$  is the rolling element diameter,  $f_i$  denotes the curvature factor of the inner race and  $f_o$  symbolizes the curvature factor of the outer race.

### 2.2 Bearing Friction Torque (T)

In addition to being important for controlling the revolving system, the frictional torque of the bearing is a critical design parameter for determining the transmitted power deficit. To fabricate the drive and actuator mechanism, frictional torque—which is created by friction between two surfaces in connection—must be appropriately computed for the pitch system. The pitch system's bearing friction torque may be computed using Equation 4 (Harris *et al.*, 2009).

$$T = \mu \frac{D_m}{2} \left( \frac{4.4M}{D_m} + 2.2F_r + F_a \right) \tag{4}$$

Where,  $D_m$  denotes the pitch diameter,  $M$  stands for the transmitted moment,  $F_r$  signifies the radial load and  $F_a$  symbolizes the axial load.

### 2.3 Static Load Factor (SF)

The proportion of the tolerable load to the real load is known as the static load factor. To ensure that there is some margin of safety concerning the static capacity, it should be larger than 1. The static load factors are analyzed using Equation 5 (Harris *et al.*, 2009).

$$SF = \left( \frac{4000}{S_{max}} \right)^2 \tag{5}$$

The maximum Hertz stress ( $S_{max}$ ) can be calculated as per Equation 6.

$$S_{max} = \frac{2Q_{max}}{\pi b l_e} \tag{6}$$

The maximum roller load ( $Q_{max}$ ) can be computed as per Equation 7.

$$Q_{max} = \left( \frac{2F_r}{z \cos \alpha} + \frac{F_a}{z \sin \alpha} + \frac{4M}{D_m z \sin \alpha} \right) \tag{7}$$

Where  $b$  is the length of the area contact formed in the roller bearing.

#### 2.4 Multi-Objective Genetic Algorithm (MOGA)

MOGA has been applied to achieve non-dominated solutions for the multi-objective design optimization of wind turbine yaw bearings. In the development of MOGA, several key steps are implemented to effectively identify optimal solutions across competing objectives. Initially, critical MOGA parameters are prepared to ensure the algorithm's operational readiness and adaptability to the problem's constraints. The process begins with the selection of a randomly generated population, which serves as the initial pool of potential solutions. Each chromosome within this population undergoes a suitability assessment to determine its alignment with predefined criteria, ensuring only viable candidates proceed further. Following this, the crossover process is executed, promoting genetic diversity and allowing for the combination of favorable traits between chromosomes. Subsequently, a mutation procedure introduces stochastic variations to maintain diversity and prevent premature convergence.

After these genetic operations, the newly generated chromosomes are evaluated for their acceptability. To further refine the selection, an ascendancy test is applied to rank the solutions, aligning them closer to the Pareto optimal front—a set of solutions where improvements in one objective would require compromises in others. This iterative process continues until a sufficient number of solutions achieve Pareto front alignment, providing a well-distributed set of trade-offs among the objectives. Finally, the decision-maker reviews the outcomes, selecting the solution that best aligns with their preferences, balancing the various objectives within the solution space (Deb, 2011). This approach ensures that the MOGA is both comprehensive in scope

and adaptable to the decision-maker's priorities, yielding robust multi-objective solutions (Bhattacharjee *et al.*, 2022).

In MOGA, the criteria for determining whether a solution is acceptable involve multiple steps that evaluate the solution's quality and its potential contribution to the population. Initially, each randomly generated chromosome (solution) is assessed based on its fitness value, which represents how well it satisfies the objectives of the optimization problem. Acceptable solutions are those that meet a certain threshold of fitness, ensuring they contribute meaningfully to the overall search process.

After the crossover and mutation processes are applied to introduce variation, the newly generated solutions are further evaluated for their suitability. These solutions undergo a selection process where only those that demonstrate a balance between exploration (diversifying the search) and exploitation (refining promising solutions) are retained. The dominance criterion, often used in MOGA, checks if a solution is non-dominated, meaning that no other solution in the population outperforms it across all objectives. Acceptable solutions are then subjected to an ascendancy test, ensuring they contribute to the formation of a Pareto optimal front. By setting these clear acceptability criteria, MOGA ensures that only high-quality, non-dominated solutions continue through the optimization process, guiding the algorithm toward the Pareto optimal front.

### *2.5 Multi-Objective JAYA Algorithm (MOJAYAA)*

The phases of the relatively new Teaching-Learning Based Optimization (TLBO) algorithm MOJAYAA, which is based on an improved Strength Pareto Evolutionary Algorithm, are discussed subsequently.

To implement an efficient multi-objective optimization process, the algorithm begins by generating a randomized initial population of solutions. Each solution is then evaluated using a defined goal function to assess its quality and effectiveness within the given objectives. Solutions are subsequently organized into distinct Pareto fronts using a non-dominated sorting technique, allowing for a clear ranking of solutions based on their objective fulfillment without outperformance by others on all objectives (Rao and More, 2017). Within each Pareto front, a crowding distance is calculated to maintain diversity, ensuring a spread of solutions across the solution space. For the next generation, solutions are selected based on a combination of their crowding distance and their rank from non-dominated sorting. Exploration and

exploitation operators are then applied to these selected solutions, promoting a balance between discovering new solution areas and refining existing high-quality solutions. This updated population retains the intended population size, ensuring consistency across generations. The algorithm continues iterating until the termination conditions are met, ultimately forming a Pareto front that represents an optimal set of trade-offs across multiple objectives (Rao and Saroj, 2017).

In MOJAYAA, the acceptability of a solution is determined through a structured evaluation process that ensures only high-quality solutions advance through the algorithm's stages. Initially, a random population of solutions is generated, and each solution is evaluated based on the objective function, which quantifies how well the solution meets the problem's goals.

After this initial evaluation, solutions are sorted into distinct Pareto fronts using non-dominated sorting. A solution is considered acceptable if it is non-dominated, meaning no other solution in the population performs better across all objectives. Once solutions are categorized, crowding distance is calculated within each Pareto front. This distance measures how close a solution is to others in the objective space, ensuring a diverse spread of solutions. Solutions with larger crowding distances are preferred as they help maintain diversity in the population.

Following these assessments, solutions are selected for the next generation based on a combination of their Pareto front ranking and crowding distance. The selected solutions then undergo exploration and exploitation processes to generate new solutions. The population is updated, ensuring that the new generation maintains the desired size while including only those solutions that meet the acceptability criteria of non-domination and diversity. Finally, the algorithm checks if the termination conditions are met; if so, the Pareto front is formed.

Thus, MOJAYAA uses a combination of non-dominated sorting, crowding distance, and solution diversity to determine which solutions are acceptable, allowing the algorithm to progress toward forming a well-distributed Pareto front.

### 3. Results and Discussion

The limitations established by Duggirala *et al.* (2018) were applied in this study, and they have been specified using Equations 8 - 18.

The bearing assembly angle ( $\phi_0$ ) has been computed as per Equation 8.

$$\phi_0 = 2\pi - 2 \cos^{-1} \left[ \frac{\left\{ \left( \frac{D-d}{2} - 3 \left( \frac{T}{4} \right) \right)^2 + \left\{ \frac{D}{2} - \left( \frac{T}{4} \right) - D_b \right\}^2 - \left\{ \frac{d}{2} + \left( \frac{T}{4} \right) \right\}^2 \right\}}{2 \left\{ \frac{D-d}{2} - 3 \left( \frac{T}{4} \right) \right\} \left\{ \frac{D}{2} - \left( \frac{T}{4} \right) - D_b \right\}} \right] \quad (8)$$

Parameter  $T$  has been computed as per Equation 9.

$$T = D - d - D_b \quad (9)$$

The bearing assembly angle is constrained as per Equation 10.

$$g_1(X) = \frac{\phi_0}{2 \sin^{-1} \left( \frac{D_b}{D_m} \right)} - z + I \geq 0 \quad (10)$$

The roller element diameter ( $D_b$ ) has been computed as the constraint function stated in Equations 11 and 12.

$$g_2(X) = 2D_b - K_{D_{min}}(D-d) \geq 0 \quad (11)$$

$$g_3(X) = K_{D_{max}}(D-d) - 2D_b \geq 0 \quad (12)$$

The bearing width ( $B$ ) is constrained as per Equation 13.

$$g_4(X) = \zeta B_w - D_b \leq 0 \quad (13)$$

$\zeta$  is a positive factor. The pitch diameter  $D_m$  has been computed as per Equations 14-16.

$$g_5(X) = D_m - (0.5 - e)(D + d) \geq 0 \quad (14)$$

$$g_6(X) = (0.5 + e)(D + d) - D_m \geq 0 \quad (15)$$

$$g_7(X) = 0.5(D - D_m - D_b) - \epsilon D_b \geq 0 \quad (16)$$

$e$  and  $\varepsilon$  are positive fractions. The internal curvature factor ( $f_i$ ) and external curvature factor ( $f_o$ ) have been computed as per Equations 17-18.

$$g_8(X) = 0.515 \leq f_i \leq 0.52 \tag{17}$$

$$g_9(X) = 0.515 \leq f_o \leq 0.53 \tag{18}$$

According to the WT yaw bearing catalog, which specifies bearings suitable for power-generating capacities ranging from 60 kW to 6.0 MW, the relevant variables, such as load capacities, rotational speed limits, bearing life, and material properties, have been carefully maintained within strict operational limits to ensure optimal performance and longevity. These variables, as outlined in Table 1, are crucial for achieving reliable and efficient power generation while minimizing wear, failure risks, and maintenance requirements over the turbine's operational lifespan.

Table 1. WT Associated Parameters and Limits (Harris *et al.*, 2009)

Parametric Limits
$B_w \sim \{30, 75\}$
$d \sim \{325, 2988\}$
$D \sim \{495, 3675\}$
$D_b \sim \{0.15(D-d), 0.26(D-d)\}$
$D_m \sim \{0.5(D+d), 0.6(D+d)\}$
$e \sim \{0.02, 0.1\}$
$f_i \sim \{0.515, 0.6\}$
$f_o \sim \{0.515, 0.6\}$
$F_a = 226 \text{ kN}$
$F_r = 46.93 \text{ kN}$
$K_{D_{\max}} \sim \{0.6, 0.7\}$
$K_{D_{\min}} \sim \{0.4, 0.5\}$
$l_e \sim \{24.4, 44\}$
$M = 217 \text{ kNm}$
$z \sim \{40, 280\}$
$\varepsilon \sim \{0.3, 0.4\}$
$\kappa \sim \{0.0758, 0.4601\}$
$\zeta \sim \{0.60, 0.85\}$

Figures 1 and 2 present the Pareto fronts obtained using MOGA. The figures provide the Pareto fronts attained for the above-mentioned objectives of the study for 45° and 60° contact angle respectively.

A population of 500 solutions and 500 generations were considered as sufficient for achieving the Pareto front based on theoretical considerations of solution diversity and problem complexity. Empirically, testing shows no significant improvements beyond this point, confirming adequate convergence and coverage of the Pareto front without excess computational cost.

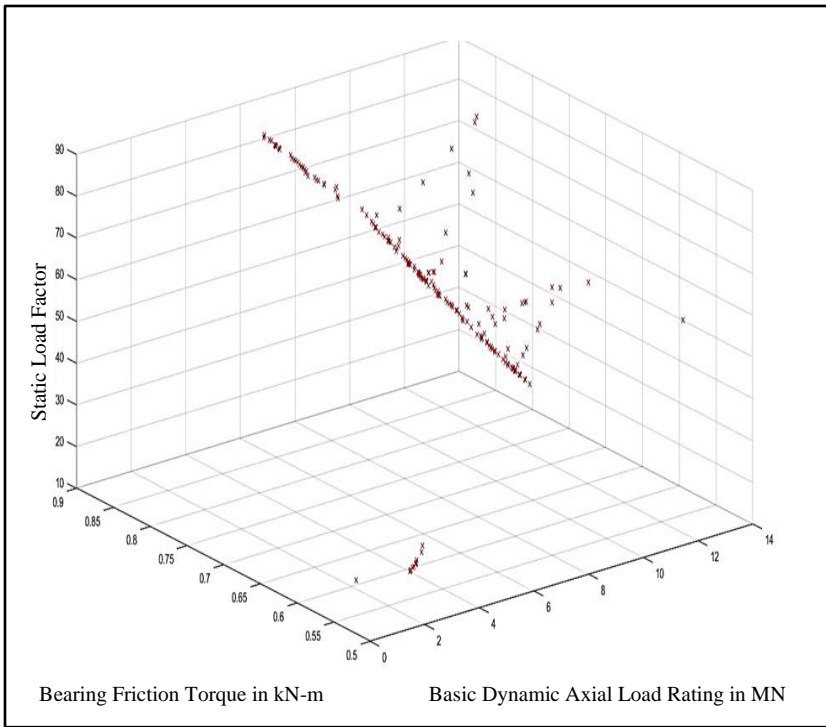


Figure 1. Pareto Front Accomplished by MOGA for 45° Contact Angle

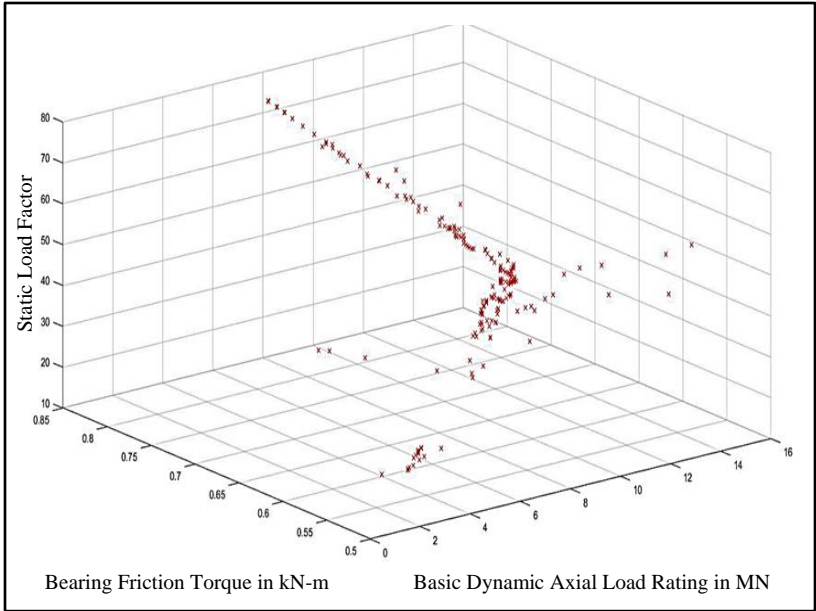


Figure 2. Pareto Front Accomplished by MOGA for 60° Contact Angle

Figures 3 and 4 display the Pareto fronts obtained with MOJAYAA. The figures provide the pareto fronts attained for the above-mentioned objectives of the study for 45° and 60° contact angle respectively.

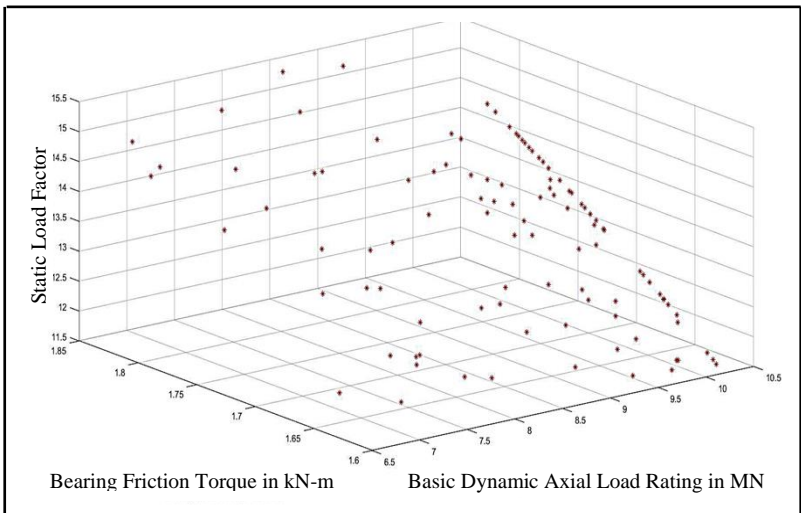


Figure 3. Pareto Front Accomplished by MOJAYAA for 45° Contact Angle

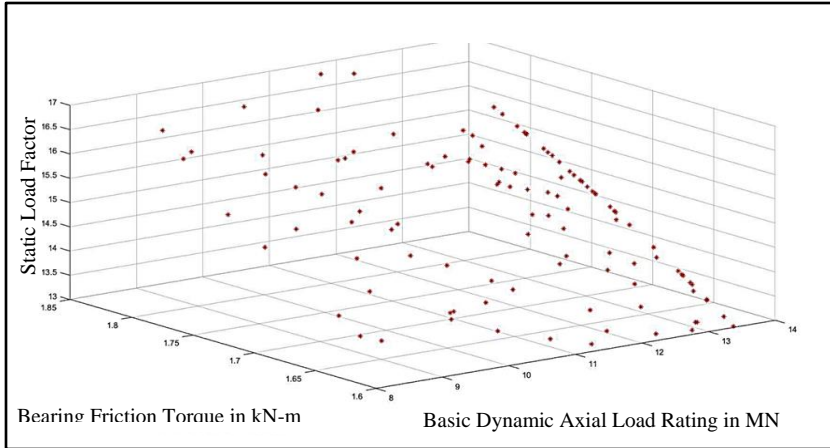


Figure 4. Pareto Front Accomplished by MOJAYAA for 60° Contact Angle

Table 2 displays the solutions that have been optimized. The analysis identifies distinct clusters where solutions are concentrated, reflecting various trade-offs between conflicting objectives, specifically for contact angles of 45° and 60°.

For the MOGA solutions at a 45° contact angle, the maximum basic dynamic axial load rating is 14 MN (Figure 1, Table 2). For 60° contact angle, it increases to 16 MN (Figure 2, Table 2). In contrast, MOJAYAA solutions yield lower basic axial load ratings of 10.18 MN for 45° contact angle (Figure 3, Table 2) and 13.21 MN for 60° contact angle (Figure 4, Table 2), indicating a stronger performance by MOGA in terms of load capacity. Furthermore, an identical minimum bearing friction torque of 0.51 kN-m is attained at both contact angles for MOGA (Figures 1 and 2, Table 2), whereas MOJAYAA solutions exhibit significantly higher values of 1.6 kN-m at both contact angles (Figures 3 and 4, Table 2), highlighting MOGA's superior efficiency.

The analysis also reveals differences in the maximum static load factor, where MOGA demonstrates values of 81 for 45° contact angle (Figures 1, Table 2) and 74 for 60° contact angle (Figure 2, Table 2). MOJAYAA offers lower values of 15.4 for 45° contact angle (Figure 3, Table 2) and 16.9 for 60° contact angle (Figure 4, Table 2). These results indicate that MOGA generally performs better in achieving higher dynamic load ratings and lower friction torques compared to MOJAYAA.

Overall, this detailed examination of the Pareto front not only elucidates the distribution and characteristics of solutions but also emphasizes the strengths of MOGA relative to MOJAYAA across the specified parameters. This information is crucial for decision-making, providing insights into the optimal configurations based on the desired trade-offs between performance metrics. A detailed analysis of the figures on Pareto fronts reveals distinct clusters or regions within the Pareto set, indicating the trade-offs between conflicting objectives in the optimization problem. These clusters highlight areas where solutions are concentrated, showing how different solutions balance the objectives of maximizing dynamic axial load rating, minimizing bearing friction torque, and maximizing static load factor.

For instance, within the Pareto front, there may be a cluster where solutions achieve higher dynamic load ratings but with a corresponding increase in bearing friction torque, reflecting a trade-off between load capacity and efficiency. Another cluster might exhibit solutions with lower friction torque, but at the expense of reduced load ratings, showcasing the competing nature of these objectives.

The regions within the Pareto front also provide insights into the diversity of solutions. Wider-spread clusters suggest a greater range of possible trade-offs, giving decision-makers more flexibility in choosing solutions that align with specific preferences. On the other hand, tighter clusters might indicate areas where few solutions meet the desired balance of objectives, signaling a more constrained set of options.

By examining these clusters and regions, the analysis helps in understanding the distribution of optimal solutions and their implications for decision-making, allowing for a clearer interpretation of the best trade-offs between the objectives being optimized.

Table 2 presents the data that demonstrate MOGA's superiority in terms of improving wind turbine yaw bearing design. The enhanced design reduces wind power generating costs while improving performance dependability.

The performance differential between MOJAYAA and MOGA may stem from differences in selection mechanisms, population diversity, and convergence speed, as well as variations in the effectiveness of crossover and mutation operators, management of non-dominated solutions, objective function complexity, parameter settings, computational efficiency, and

problem-specific features. These factors collectively influence how each algorithm navigates the solution space and forms the Pareto front.

Table 2. Comparative Outcomes between MOGA and MOJAYAA

	MOGA Solution		MOJAYAA Solution	
	45° Contact Angle	60° Contact Angle	45° Contact Angle	60° Contact Angle
Maximum Basic Dynamic Axial Load Rating in MN	14	16	10.18	13.21
Minimum Bearing Friction Torque in kN-m	0.51	0.51	1.6	1.6
Maximum Static Load Factor	81	74	15.4	16.9

The present research work significantly enhances engineers' ability to select optimal design alternatives by identifying distinct solution clusters within the Pareto front. These clusters highlight trade-offs between objectives like dynamic load capacity, friction torque, and static load factor, offering insights into potential design configurations. By demonstrating that MOGA achieves higher dynamic load ratings and lower friction torques compared to MOJAYAA, this research validates the effectiveness of AI in refining design choices. Furthermore, the study showcases how AI-driven techniques expedite decision-making by presenting a diverse range of solutions within the Pareto front. The clustered distribution provides engineers with clear options based on specific performance criteria, enabling more efficient and targeted engineering decisions.

This research work surpasses existing literature by introducing a novel combination of objectives that includes maximizing dynamic axial load ratings, minimizing bearing friction torque, and optimizing static load factors—each critical for high-performance bearing design (Kim and Dalhoff, 2014). Unlike traditional studies that often focus on single or limited objective optimization, this research adopts a multi-objective approach that captures the complex trade-offs inherent in engineering applications (Harris *et al.*, 2009).

Additionally, the application of advanced AI-driven metaheuristic techniques, particularly MOGA, represents a leap forward in optimization efficiency and solution quality. While previous studies typically employ standard optimization methods, this work demonstrates that MOGA outperforms

alternative methods (e.g., MOJAYAA) in achieving higher load capacities and lower friction torques (Nam *et al.*, 2016). The innovative integration of these objectives and advanced algorithms highlights this research's contribution to more precise and versatile design optimization, setting a new standard in the field (Xu *et al.*, 2021).

#### **4. Conclusion and Recommendation**

By improving WT yaw bearing design, the study aimed to increase the performance of a wind power production system. To maximize the taken into consideration objectives, MOGA and MOJAYAA have been utilized. According to the study, MOGA is more effective than MOJAYAA for the current research work. Other AI techniques could be applied in the future to enhance the WT yaw bearing's design. In addition, other WT components may be taken into account for AI-based design optimization.

#### **5. Acknowledgement**

The first author thanks Jadavpur University for helping to sponsor this research effort.

#### **6. References**

- Babu, J. & Jithesh, S. (2008). Breakdown risks in wind energy turbines. *Pravartak, the journal of Insurance and risk Management from National Insurance Academy, Pun*, 3(3).
- Bhattacharjee, P., Jana, R., & Bhattacharya, S. (2022). Improving the Yearly Profit of Wind Farm with Artificial Intelligence Technique. *Mindanao Journal of Science and Technology*, 20(2).
- Deb, K. (2011). Multi-objective Optimisation Using Evolutionary Algorithms: An Introduction. *Multi-Objective Evolutionary Optimisation for Product Design and Manufacturing*, 3-34. doi:10.1007/978-0-85729-652-8\_1
- Duggirala, A., Jana, R., Shesu, R., & Bhattacharjee, P. (2018). Design optimization of deep groove ball bearings using crowding distance particle swarm optimization. *Sādhanā*, 43(1). doi:10.1007/s12046-017-0775-9

Echavarría, E., Hahn, B., Van Bussel, G., & Tomiyama, T. (2008). Reliability of Wind Turbine Technology Through Time. *Journal of Solar Energy Engineering*, 130(3). doi:10.1115/1.2936235

Energy Institute. (2023). Energy Institute - Statistical Review of World Energy (2023). Retrieved 12 31, 2023, from Energy Institute: <https://www.energyinst.org/statistical-review>

Gupta, S., Tiwari, R., & Nair, S. (2007). Multi-objective design optimisation of rolling bearings using genetic algorithms. *Mechanism and Machine Theory*, 42(10), 1418–1443. doi:10.1016/j.mechmachtheory.2006.10.002

Harris, T., Rumbarger, J., & Butterfield, C. (2009). Wind Turbine Design Guideline DG03: Yaw and Pitch Rolling Bearing Life.

International Energy Agency. (2021). Global Energy Review 2021. Retrieved July 30, 2021, from International Energy Agency: <https://www.iea.org/reports/global-energy-review-2021/renewables>

Kim, M. & Dalhoff, P. (2014). Yaw Systems for wind turbines—Overview of concepts, current challenges and design methods. *Journal of Physics: Conference Series*, 524(1), 012086. doi:10.1088/1742-6596/524/1/012086

Micha, P.T., Mohan, T., & Sivamani, S. (2017). Design and Analysis of a Permanent Magnetic Bearing for Vertical Axis Small Wind Turbine. *Energy Procedia*, 117, 291-298. doi:10.1016/j.egypro.2017.05.134

Nam, J., Park, Y., & Chang, H. (2016). Dynamic life prediction of pitch and yaw bearings for wind turbine. *Journal of Mechanical Science and Technology*, 30, 249-256. doi:10.1007/s12206-015-1228-1

Obama, B. (2017). The irreversible momentum of clean energy. *Science*, 355(6321), 126-129. doi:10.1126/science.aam6284

Rao, R. & More, K. (2017). Design optimization and analysis of selected thermal devices using self-adaptive Jaya algorithm. *Energy Conversion and Management*, 140, 24-35. doi:10.1016/j.enconman.2017.02.068

Rao, R. & Saroj, A. (2017). A self-adaptive multi-population based Jaya algorithm for engineering optimization. *Swarm and Evolutionary computation*, 37, 1-26. doi:10.1016/j.swevo.2017.04.008

Rommel, D., Di Maio, D., & Tinga, T. (2020). Calculating wind turbine component loads for improved life prediction. *Renewable Energy*, 146, 223-241. doi:10.1016/j.renene.2019.06.131

Tavner, P.J., Xiang, J., & Spinato, F. (2005). Improving the reliability of wind turbine generation and its impact on overall distribution network reliability. 18th International Conference on Electricity Distribution (CIRED 2005). doi:10.1049/cp:20051199

United Nations. (2015). The Paris Agreement. Retrieved May 2, 2022, from UNFCCC: [https://unfccc.int/files/essential\\_background/convention/application/pdf/english\\_paris\\_agreement.pdf](https://unfccc.int/files/essential_background/convention/application/pdf/english_paris_agreement.pdf)

Van Bussel, G. & Zaijer, M. (2001). Reliability, availability and maintenance aspects of large-scale offshore wind farms, a concepts study. Proceedings of MAREC, 2001.

Wu, Z. & Wang, H. (2012). Research on Active Yaw Mechanism of Small Wind Turbines. Energy Procedia, 16, 53–57. doi:10.1016/j.egypro.2012.01.010

Xu, J., Benson, S., & Wetenhall, B. (2021). Comparative analysis of fatigue life of a wind turbine yaw bearing with different support foundations. Ocean Engineering, 235, 109293. doi:10.1016/j.oceaneng.2021.109293

Yang, M., Chengbing, H., & Xinxin, F. (2012). Institutions Function and Failure Statistic and Analysis of Wind Turbine. Physics procedia, 24, 25-30. doi:10.1016/j.phpro.2012.02.005